Subsurface flow and vegetation patterns in tidal environments

Nadia Ursino,[1] Sonia Silvestri,[2,3] and Marco Marani[1,3]

Received 18 August 2003; revised 16 February 2004; accepted 29 March 2004; published 28 May 2004.

[1] Tidal environments are characterized by a complex interplay of hydrological, geomorphic, and biological processes, and their understanding and modeling thus require the explicit description of both their biotic and abiotic components. In particular, the presence and spatial distribution of salt marsh vegetation (a key factor in the stabilization of the surface soil) have been suggested to be related to topographic factors and to soil moisture patterns, but a general, process-based comprehension of this relationship has not yet been achieved. The present paper describes a finite element model of saturated-unsaturated subsurface flow in a schematic salt marsh, driven by tidal fluctuations and evapotranspiration. The conditions leading to the establishment of preferentially aerated subsurface zones are studied, and inferences regarding the development and spatial distribution of salt marsh vegetation are drawn, with important implications for the overall ecogeomorphological dynamics of tidal environments. Our results show that subsurface water flow in the marsh induces complex water table dynamics, even when the tidal forcing has a simple sinusoidal form. The definition of a space-dependent aeration time is then proposed to characterize root aeration. The model shows that salt marsh subsurface flow depends on the distance from the nearest creek or channel and that the subsurface water movement near tidal creeks is both vertical and horizontal, while farther from creeks, it is primarily vertical. Moreover, the study shows that if the soil saturated conductivity is relatively low (10^{-6} m s^{-1}, values quite common in salt marsh areas), a persistently unsaturated zone is present below the soil surface even after the tide has flooded the marsh; this provides evidence of the presence of an aerated layer allowing a prolonged presence of oxygen for aerobic root respiration. The results further show that plant transpiration increases the extent and persistence of the aerated layer, thereby introducing a strong positive feedback: Pioneer plants on marsh edges have the effect of increasing soil oxygen availability, thus creating the conditions for the further development of other plant communities. *INDEX TERMS:* 1875 Hydrology: Unsaturated zone; 1851 Hydrology: Plant ecology; 1890 Hydrology: Wetlands; 1866 Hydrology: Soil moisture; *KEYWORDS:* tidal environments, ecohydrology

Citation: Ursino, N., S. Silvestri, and M. Marani (2004), Subsurface flow and vegetation patterns in tidal environments, *Water Resour. Res.*, *40*, W05115, doi:10.1029/2003WR002702.

1. Introduction

[2] Tidal environments are dynamic and delicate systems exposed to the effects of climatic changes and often subject to increasing human pressure. The biological and socioeconomic importance of intertidal areas, recognized by international conventions (such as the Ramsar Convention), and their role as buffer zones between land and sea have stimulated a renewed scientific interest for their dynamics [e.g., *Fagherazzi et al.*, 1999; *Rinaldo et al.*, 1999a, 1999b; *Allen*, 2000; *Friedrichs and Perry*, 2001; *Marani et al.*, 2002; *Fagherazzi et al.*, 2003; *Marani et al.*, 2003, 2004]. A deep understanding of the morphogenesis and evolution of tidal environments requires an interdisciplinary approach incorporating the description of the strong coupling between biological and physical processes. Biological and hydrological/geomorphological dynamics in salt marshes are in fact so strongly interacting that successful models of intertidal systems must explicitly incorporate the description of both their living and nonliving components. One important example of such strong coupling is the feedback between vegetation and tidal marsh hydrology and topography from which the present paper takes its main motivation.

[3] Halophytic vegetation, i.e., plant species which have adapted to living in salty environments, plays a central role in determining the stability of tidal marshes. Vegetation, in fact, stabilizes marsh surface sediments; increases friction to hydrodynamic flow and reduces water sediment transport capacity, thereby favoring sediment deposition; and inhibits the formation of wind-induced waves which cause sediment resuspension. In turn, vegetation development is strongly linked to the topographic characteristics of the marsh, creating a strong link between geomorphic structures and

[1]Dipartimento di Ingegneria Idraulica, Marittima, Ambientale e Geotecnica, Università di Padova, Padua, Italy.
[2]Servizio Informativo del Consorzio Venezia Nuova, Magistrato alle Acque di Venezia, Venice, Italy.
[3]Centro Internazionale di Idrologia "D. Tonini," Università di Padova, Padua, Italy.

0043-1397/04/2003WR002702$09.00

vegetation distribution. In fact, it has been shown that halophytic vegetation is spatially organized in patches, producing a characteristic spatial distribution called zonation [*Silvestri et al.*, 2000; *Pignatti*, 1966; *Chapman*, 1964]. Species distribution has often been found to be strongly correlated to topographic elevation [*Sanchez et al.*, 1996; *Adam*, 1990; *Olff et al.*, 1988; *Vince and Snow*, 1984; *Snow and Vince*, 1984; *Mahall and Park*, 1976], and its typically clustered organization is usually ascribed to differences in the duration of submersion periods corresponding to different soil elevations [*Rogel et al.*, 2001; *Levine et al.*, 1998; *Cantero et al.*, 1998; *Pignatti*, 1966]. These differences are often characterized by defining the hydroperiod [*Kadlec and Knight*, 1996], i.e., the ratio between the length of time during which a given marsh area is submerged to the total duration of the period of reference (usually 1 year or the growing season). Other authors [*Olff et al.*, 1988] also consider the tidal inundation frequency on salt marsh vegetation and find a correlation with species distribution patterns.

[4] Recent results contradict this simplified view. *Silvestri* [2000] and *Silvestri et al.* [2004], in fact, show that an identical succession of vegetation species with increasing soil elevation is observed on different salt marshes within the same tidal embayment, but a given species is found at preferential elevations which differ from one marsh to another: The same plant succession is shifted vertically at different sites. Using a hydrodynamic model to account for tidal propagation, they further show that no clear correlation may be established between vegetation species and submersion periods, thus questioning the traditional idea that halophytic vegetation simply responds to the hydroperiod.

[5] The distribution of halophytes may thus respond not to simple rules dictated by the tidal cycle but rather to a combination of two or more factors, likely linked to the groundwater system. In particular, the development of salt marsh vegetation may be linked to the existence and duration of an unsaturated layer allowing aerobic root respiration. In fact, even though wetland plants present a number of physiological characteristics that enable them to survive periodic soil saturation and the related changes in soil chemistry (e.g., aerenchyma, a network of intercellular spaces connecting the tissues of the roots to the aboveground parts [*Visser et al.*, 2000]), plant aerobic respiration through their roots remains crucial for their establishment and development [*Chapman*, 1960; *Mendelssohn et al.*, 1981; *Armstrong*, 1982; *Pezeshki*, 2001].

[6] The existence and persistence of an aerated layer under the soil surface have been a source of contrasting positions in the scientific literature: Some authors [e.g., *Chapman*, 1960, 1964; *Pezeshki*, 2001] assign an important role to an aerated soil layer for the aerobic respiration of the roots, while others [e.g., *Armstrong et al.*, 1985] even doubt an unsaturated layer exists. Using soil redox potential as an indicator of soil aeration in the top 30 cm layer, *Howes et al.* [1981] found that in the Great Sippewissett salt marsh (Cape Code, Massachusetts), sediments near creeks are more oxidized than those in the inner marsh areas. Below the topsoil layer, under the root zone, *Howes et al.* find no significant difference between the redox potential measured near or far from creeks. To summarize, it may be concluded that most authors agree that higher salt marsh soils are characterized by longer periods of oxidation, but the link to the relevant hydrologic and morphologic factors (e.g., distance from creeks, hydraulic conductivity, evapotranspiration) have not yet been clearly established nor studied on a quantitative basis. In order to fill this gap and to fully comprehend the interaction between marsh hydrology, geomorphology, and vegetation dynamics, a description of subsurface flow is required.

[7] This paper introduces a process-based description of the interplay between vegetation and soil moisture dynamics by using a finite element model of saturated and unsaturated subsurface flow, in a schematic salt marsh, driven by tidal fluctuations and evapotranspiration. A space-dependent subsurface aeration time is defined and evaluated through numerical experiments, and the conditions leading to the existence of a root aeration zone are analyzed. A schematic, representative cross section of a flat salt marsh between two streams is considered. The simulations cover a range of parameter variability typical of many tidal environments (e.g., the Venice lagoon [*Simonini and Cola*, 2002; *Alvarez Rogel et al.*, 2001]) and are focused on threshold values of conductivity and evapotranspiration that determine very different space-time organizations of the aeration zones. Indeed, the cases explored in the present study clearly provide evidence of the role of saturated hydraulic conductivity and of evapotranspiration in determining different soil moisture and aerated soil layer patterns.

2. Salt Marsh Subsurface Water Flow

[8] Groundwater level fluctuations in response to a tidal forcing were investigated by several previous authors [e.g., *Sun*, 1997; *Jiao and Tang*, 1999; *Li et al.*, 2000; *Li and Jiao*, 2002], but there is a distinctive lack of studies incorporating both saturated and unsaturated flow, which is a crucial factor in determining subsurface water dynamics in areas subject to tidal inundations, such as salt marshes. Solving water flow within saturated and unsaturated zones provides the time-dependent pressure head (and the corresponding degree of saturation) over the whole profile of interest. Since a most important factor determining plant development is the length of time during which the soil is unsaturated, the numerical modeling of subsurface flow allows the quantitative study of moisture patterns which are a key factor in marsh ecohydrological dynamics.

[9] Water flow in salt marsh soils was studied by integrating Richards' equation,

$$\nabla[K(\Psi)\nabla(\Psi + z)] = \frac{\partial \theta}{\partial t}, \tag{1}$$

where $K(\Psi)$ is the pressure-dependent unsaturated soil conductivity, Ψ is the negative pressure head, z is the vertical coordinate (positive upward), θ is the water content, and t is time. We assume exponential constitutive relations for the conductivity and the water retention curve that express the relationship between conductivity, water content, and pressure head [*Gardner*, 1958],

$$K(\Psi) = K_s e^{\alpha \Psi} \tag{2}$$

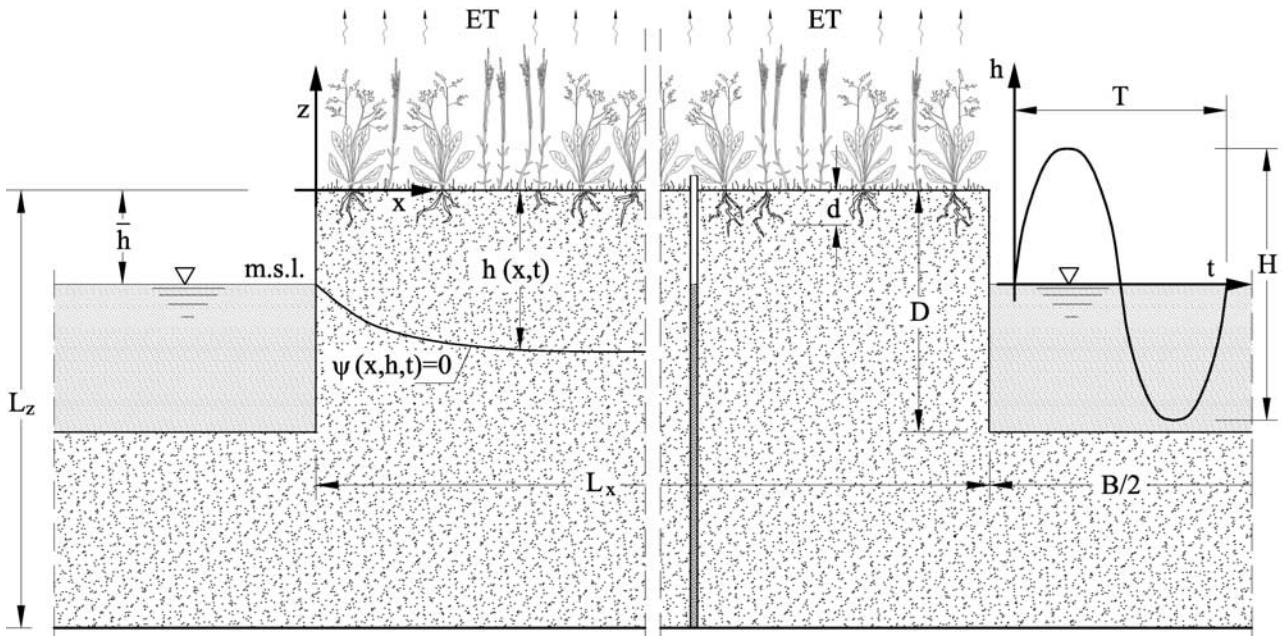

Figure 1. Schematic representation of a cross section of the model salt marsh considered. The horizontal dimensions have been multiplied by a factor of 3 with respect to the vertical scale. The imposed tidal cycle is represented in the channel on the right.

and

$$\theta = (\theta_s - \theta_r)e^{\alpha\Psi} + \theta_r, \tag{3}$$

where K_s is the saturated hydraulic conductivity, α is the inverse of the mean capillary rise, and θ_s and θ_r are the saturated and residual water content, respectively. Equations (2) and (3) hold for $\Psi < 0$. When $\Psi \geq 0$, then $K = K_s$ and $\theta = \theta_s$. An exponential relationship between K_s and Ψ and between θ and Ψ is a common assumption for analytical solutions in simple deterministic and first-order stochastic analyses of unsaturated media (see, e.g., *Yeh* [1998] and *Russo* [1998] for a review). The applicability of this hypothesis is extensively discussed by *Pullan* [1990] and *Philip* [1969]. Even though the exponential relations (2) and (3) do not accurately represent real soils when applied to wide ranges of the degree of saturation, they reproduce the basic dynamics of soil moisture and may be considered a good fit to real soil behavior when soil water content varies within a small interval. This requirement is certainly met in the salt marshes on which the design of the model system used below is based, since the degree of saturation varies between 0.8 and 1.0 in the conditions considered in the simulations. The soundness of the approach adopted was also tested by comparing results from the model using equations (2) and (3) to those obtained using van Genuchten relationships [*van Genuchten*, 1980] (comparison not shown for brevity): The results were entirely consistent and lead to the same space-time dynamics described in section 3. The Gardner model is thus chosen as it introduces fewer parameters to be explored and in view of further possible dimensional analyses and analytic developments.

[10] We numerically solve equation (1) coupled to equations (2) and (3) using a finite element approach. The geometry of the domain used to represent a typical marsh subject to tidal fluctuations is shown in Figure 1 and consists of a rectangular cross section of the salt marsh lying between two channels. The soil is assumed to be homogeneous and isotropic. The soil depth from the marsh surface to the impermeable layer is $L_z = 2.5$ m. As shown in Figure 1, B is the channel width and L_x is the marsh width from channel to channel. We assume $L_x = 10$ m and $B = 1$ m; $\bar{h}$ represents the marsh elevation with respect to the mean sea level. We will consider two cases, $\bar{h} = 0.6$ m above sea level (asl) and $\bar{h} = 0.3$ m asl, the different elevations leading to different hydroperiods. The tidal oscillation is simply sinusoidal with amplitude $H = 2$ m and period $T = 12$ hours. The geometric setup for the marsh and the tidal forcing was chosen to mimic typical situations observed in microtidal lagoons, such as the lagoon of Venice (Italy) [*Silvestri et al.*, 2000, 2004]. Since the geometry of the system, and thus the flow patterns, is symmetric, just half of the domain is considered in the computations, extending from the axis of the left channel to the middle cross section of the marsh, where a no flux lateral boundary condition is imposed.

[11] The forcing imposed by tidal fluctuations is simulated by assigning a time-dependent hydrostatic pressure profile as a boundary condition in the channel. The boundary condition on the surface of the marsh varies in time from a positive, time-dependent pressure head (when the tidal level is such that water floods the salt marsh) to a fixed value of the vertical water flux: This is equal to zero in the absence of vegetation or equal to a uniform and constant evapotranspiration ET otherwise. It should here be noted that the presence of vegetation could be modeled in greater detail by use of more refined representations of water uptake at the scale of single roots [e.g., *Vrugt et al.*, 2001]. Nevertheless, this approach would add to the complexity of the model by introducing new parameters, without changing the overall characteristics of the solution at

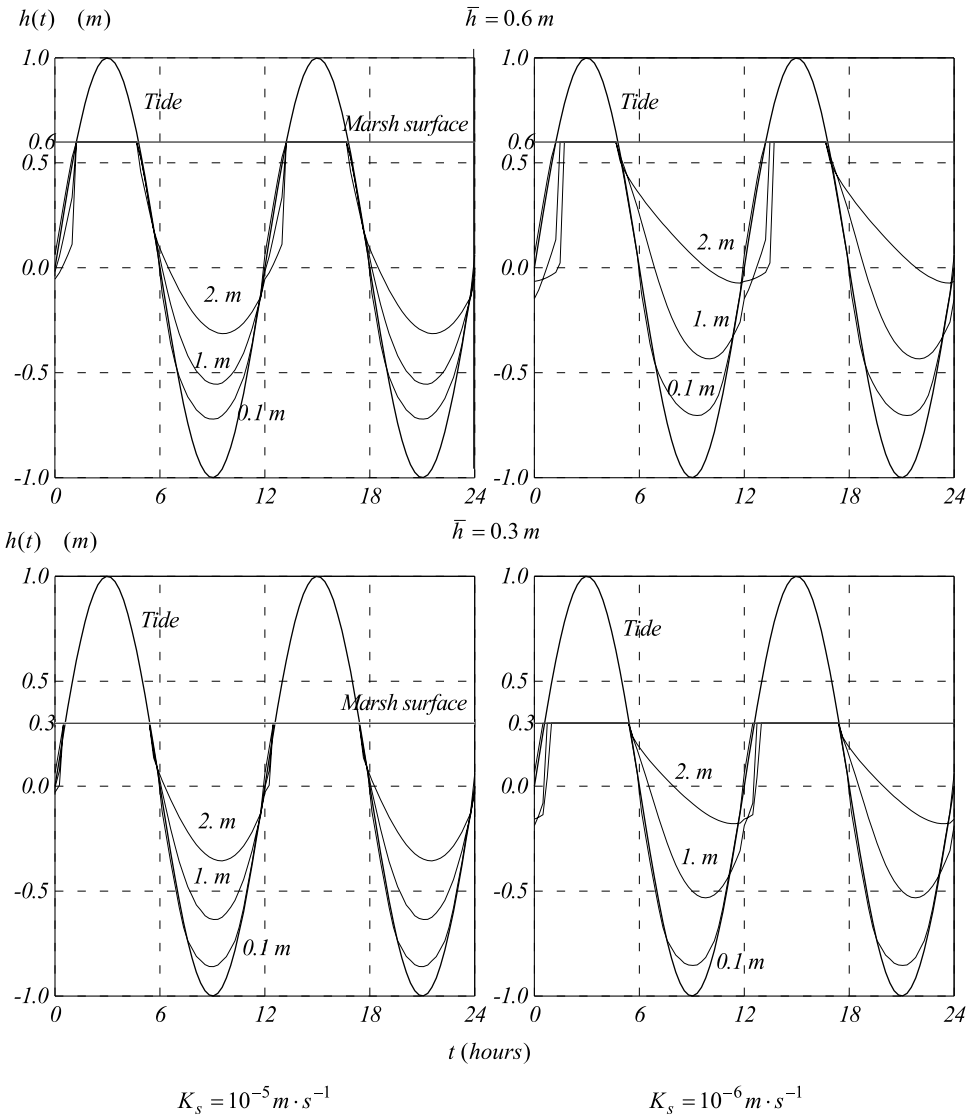

Figure 2. Sea level and water table fluctuation at different distances from the channel (expressed in meters from the channel).

scales larger than a single plant. The lower boundary condition prescribes a constant pressure head $\Psi = L_z - \bar{h}$. This is based on the assumption that at some depth the pressure head tends to be insensitive to tidal fluctuations and thus assumes the hydrostatic value corresponding to the mean sea level.

3. Results

[12] A series of simulations has been run for different marsh elevations $\bar{h}$ and different vegetation densities (corresponding to different *ET* values), obtaining the "equilibrium" pressure head distribution $\Psi(x, z, t)$, after a sufficient number of tidal cycles to allow the system to lose memory of the initial conditions and to allow for its evolution to become periodic. The results within one cycle are then recorded with time step $\Delta t = 15$ min.

[13] The numerical experiments were performed for two realistic values of the saturated hydraulic conductivity, $K_s = 10^{-5}$ m s^{-1} and $K_s = 10^{-6}$ m s^{-1}, within the range of variability found in many tidal environments [e.g., *Simonini and Cola*, 2002]. The remaining soil parameters were kept constant: $\theta_r = 0.06$, $\theta_s = 0.4$, and $\alpha = 0.1$ m^{-1} (value assuring the convergence of the numerical model, while realistically reproducing soil behavior under the critical wetting/drying conditions).

[14] It is worth noting here that the objective of the model developed is the identification of possible different subsurface flow regimes and patterns within tidal salt marshes under the most general possible assumptions; the use of soil parameters and of a geometrical setup typical of real tidal marshes is thus needed, as opposed to the detailed description of a specific salt marsh.

[15] All simulations presented below refer to the same distance between the channels $L_x = 10$ m. Larger values of L_x were explored, and it was found that the pressure conditions in the inner part of the marsh become independent of tidal fluctuations in the channel for sufficiently large values of L_x. The assumption of $L_x = 10$ m leads, for the typical salt marsh soil characteristics assumed, to a "wide marsh," in which the tidal forcing does not influence the inner part of the marsh. As a consequence, the flow field is

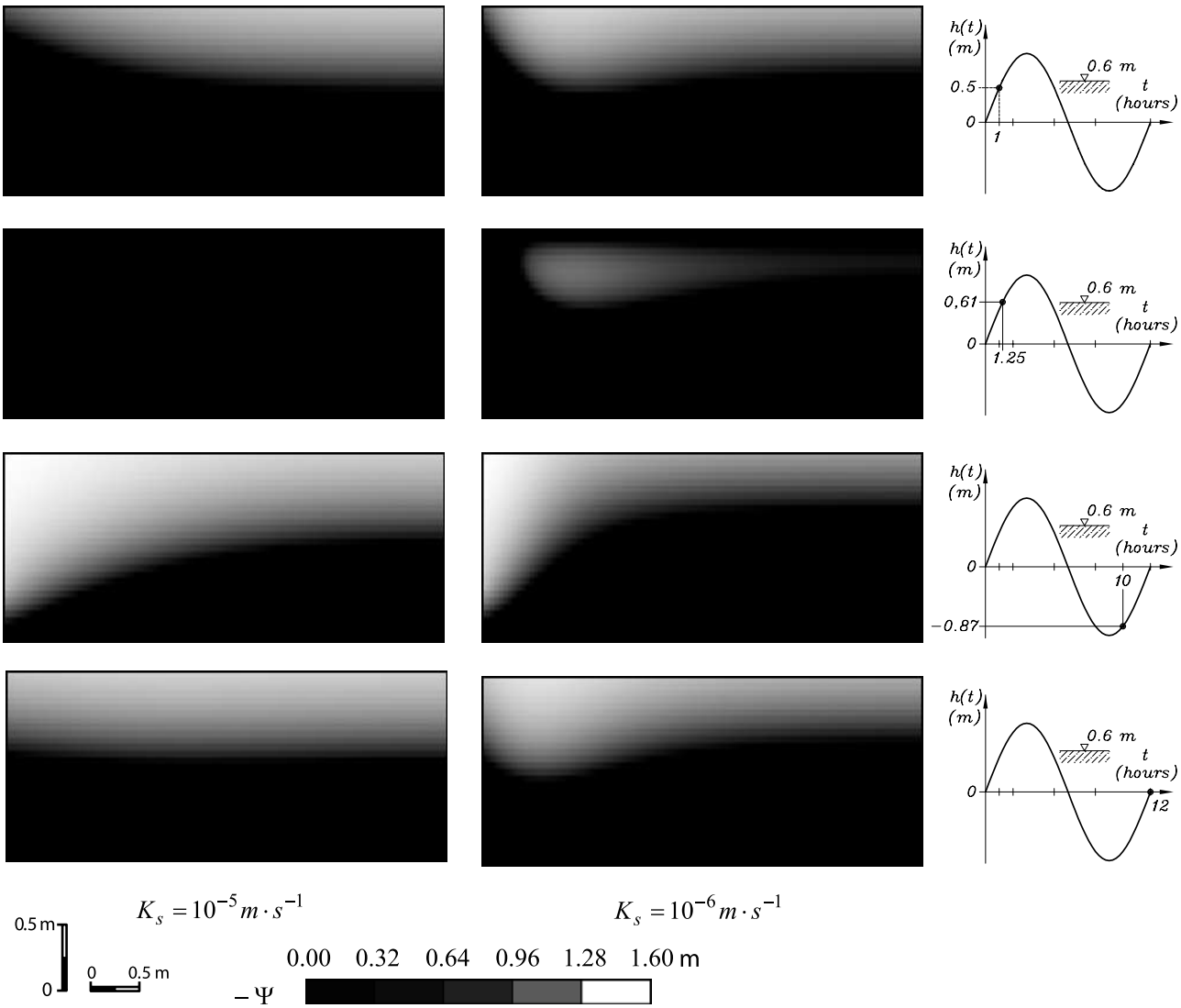

Figure 3. Time evolution of the pressure head distribution within the left half of the schematic marsh represented in Figure 1, for nonvegetated marsh (ET = 0). Black indicates saturated regions (positive pressure head), whereas lighter shades of gray indicate increasingly aerated zones (more negative pressure head).

two-dimensional (horizontal and vertical) close to the creek, where it is influenced by the tidal oscillations, and one-dimensional (vertical) far from it, in the middle of the marsh.

3.1. Groundwater Fluctuations

[16] Tidal groundwater level oscillations are easily derived from pressure head distributions, since the condition $\Psi(x, h, t) = 0$ identifies the water table $h(x, t)$ (Figure 1). Figure 2 illustrates the fluctuations of the water table induced by the tide with amplitude H = 2 m at different distances from the channel: x = 0.1, 1.0, and 2.0 m. The plots refer to the cases of mean marsh elevation $\bar{h}$ = 0.6 m asl (Figure 2, top) and $\bar{h}$ = 0.3 m asl (Figure 2, bottom) and saturated conductivity $K_s = 10^{-5}$ m s^{-1} (Figure 2, left) and $K_s = 10^{-6}$ m s^{-1} (Figure 2, right). The evapotranspiration is set to ET = 0 mm/day.

[17] At a greater distance from the channel the water table is less influenced by negative tidal fluctuations because of the damping effect of the soil, whereas in the rising limb of the tidal forcing, as soon as the water floods the marsh, infiltration from above comes into play, efficiently recharging the soil throughout the marsh. The superposition of the two mechanisms thus leads to higher groundwater levels toward the center of the marsh.

[18] Figure 2 shows that this effect is clearly more pronounced within the less conductive marsh. Further, the system exhibits a greater inertia with respect to water inflow from the channel as compared with water drainage to it. This is evident from the retarded response to the rising tide in the inner part of the marsh and from the resulting asymmetry of the groundwater table oscillation. This is most apparent when one compares, for x = 2 m, Figure 2 (right) with Figure 2 (left).

3.2. Pressure Head Distributions

[19] The pressure head distribution is plotted in Figure 3 at different times to show the shape and persistence of the aerated zone within the soil profile. The lower part of the

marsh, where the pressure head is always positive, has not been represented, and only 1.4 m below the marsh surface are shown. The vertical scale is stretched to improve the readability. The ratio between the vertical and the horizontal scales is 1.5.

[20] Figure 3 shows the history of the pressure head distribution within a marsh with mean elevation $\bar{h}$ = 0.6 m asl. Figure 3 (left images) represents the evolution of the pressure head at four different times for K_s = 10^{-5} m s^{-1} (more conductive marsh). Figure 3 (right images) shows the evolution of the pressure head distributions for a less conductive marsh ($K_s = 10^{-6}$ m s^{-1}). The flux on the marsh surface (evapotranspiration) is set to $ET = 0$ m d^{-1} in both cases.

[21] Figure 3 shows that the development and characteristics of the aeration zone are substantially different when hydraulic conductivity is changed. In the more conductive marsh, water is more mobile. When water floods the marsh, infiltration from above takes place and quickly saturates the marsh completely.

[22] In the less conductive marsh the influence of the creek is confined to a smaller area in its vicinity. The maximum depth of the aerated layer is reached when the sea level is at its minimum (Figure 2), then the channel starts recharging the marsh as the sea level rises again. Figure 3 (right images) demonstrates that water from the channel hardly penetrates into the inner sections of the less conductive marsh, leading to a characteristic convexity of the lower boundary of the aerated layer. A persistent minimum of the water table at a short distance from the creek (see cases for t = 12 hours and t = 1 hours) is observed. The presence of this minimum is due to the fact that the water table fluctuations in the middle of the marsh lag behind fluctuations of water levels in the creek channel because of the relatively low mobility of the water in this case. Hence, when the water level is rising from the tidal minimum in the creek, the water table in the middle of the marsh is still draining toward it. A minimum in the water table is thus located in the area of transition between the creek and the inner marsh. When the marsh is flooded, a wetting front penetrates from above, but an unsaturated layer below the soil surface (t = 1.25 hours) persists in the less conductive marsh, leading to prolonged aeration periods for vegetation roots.

[23] We now turn to addressing the effects of a uniform vegetation cover, represented by a uniform evapotranspiration flux leaving the surface of the marsh when it is not flooded. We have experimented with various values of evapotranspiration within representative ranges observed for salt marsh vegetation [*Dacey and Howes*, 1984]. For brevity, only results for ET = 4 mm d^{-1} are presented. These were found to be representative of the general behavior. The pressure head distributions are plotted in Figure 4.

[24] In general, a positive ET causes, as expected, lower pressure head values and thus lower saturation degrees and larger and more persistent aerated zones than in the case of ET = 0 mm d^{-1}. A comparison between the cases of ET = 0 mm d^{-1} and ET = 4 mm d^{-1} for the highly conductive marsh (Figures 3 and 4, left images) indicates that the cross sections of the salt marsh characterized by deeper aeration layers are roughly the same. On the other hand, major differences may be seen in the behavior of the less conductive marsh with and without vegetation. In fact, in Figure 4 (right images) a deeper unsaturated zone extends to the middle of the marsh and persists long after the water level has risen above the marsh surface (notice that $h(t = 2$ hours) = 0.26 m). Once more, the aerated layer may exist only in a soil with low conductivity. As opposed to the nonvegetated marsh, where the unsaturated layer was found close to the creek, in the vegetated marsh the unsaturated layer is located in the inner part where the exfiltration caused by the presence of the vegetation is capable of sustaining the aerated layer against vertical infiltration when the infiltration velocity is small enough, that is, when hydraulic conductivity is small enough.

3.3. Aeration Times

[25] The pressure head maps obtained by integrating Richards' equation may be used to evaluate synthetic parameters to be introduced in ecological models for plant colonization and growth. The aeration time $t_d(x)$ is here defined as the time of persistence of unsaturated conditions within a tidal cycle at a certain depth d as a function of the distance x from the nearest channel. High values of $t_d(x)$ identify a preferential aeration zone, where possibly natural plant colonization may start, or artificial plant colonization may have a greater probability of success. The reference depth d (Figure 1) may be related to the mean root depth of plants that typically colonize a natural marsh or that may be employed for the colonization of an artificial marsh. In this section we study the function $t_d(x)$ for d = 0.10 m and d = 0.30 m and for $0 < x \leq 3$ m.

[26] Figure 5 compares the aeration times $t_{10}(x)$ and $t_{30}(x)$ for two "high" marshes ($\bar{h} = 0.6$), with $K_s = 10^{-5}$ m s^{-1} and $K_s = 10^{-6}$ m s^{-1} and for ET = 0, 2, and 4 mm d^{-1}. In the marsh with a higher soil conductivity the "shallower" aeration time t_{10} does not depend on ET, nor on x, showing that there are no preferential aeration zones at shallow depths within the marsh. Deeper in the soil, when d = 0.30 m, aeration times of the zone near the channel are very much influenced by tidal fluctuations. The aeration of the soil presents a minimum at the marsh edge, and it increases with the distance from the channel. It is seen that when the conductivity is high, aeration times near the surface (d = 0.10 m) are always higher than aeration times in the deeper layers (at d = 0.30 m).

[27] The influence of ET on the aeration times becomes more important in the less conductive marsh. When K_s = 10^{-6} m s^{-1}, both t_{10} and t_{30} increase with ET, and the increment is particularly important for $d = 0.30$ m, eventually producing an inversion of the relationship between t_{10} and t_{30}: For ET = 4 mm d^{-1}, in fact, $t_{10} < t_{30}$ in the inner marsh, indicating that deeper layers of the soil are in this area characterized by longer aeration times than shallower ones. This is due to the presence of the aerated layer discussed in section 3.2 (see Figure 4), which does not extend to the upper soil layer and thus causes a preferential aeration in deeper layers. When $ET = 0$ mm d^{-1} and $d = 0.30$ m, the area with higher aeration times is located near the channel. When ET increases, the more aerated zone migrates from the areas near the channel to the central area of the marsh.

[28] Figure 6 shows the aeration times of a marsh with mean soil elevation $\bar{h}$ = 0.3 m asl. As in Figure 5, aeration times $t_{10}(x)$ and $t_{30}(x)$ are plotted as a function of

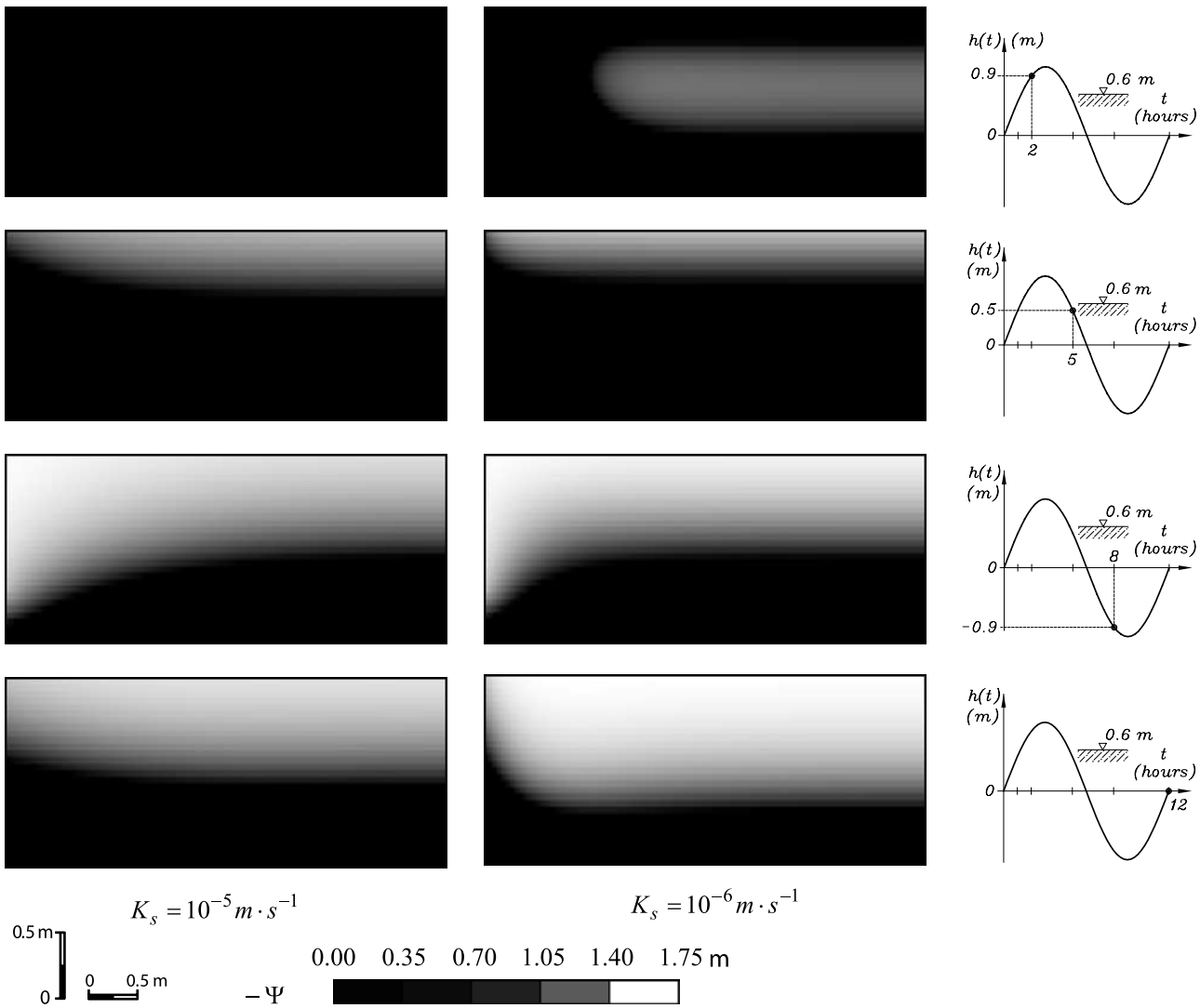

Figure 4. Time evolution of the pressure head distribution within the left half of the schematic marsh represented in Figure 1, for vegetated marsh with uniform evapotranspiration ET = 4 mm d^{-1}. Black indicates saturated regions (positive pressure head), whereas lighter shades of gray indicate increasingly aerated zones (more negative pressure head).

the distance from the channel. The conductivity is K_s = 10^{-5} m s^{-1} (Figure 6, left) and $K_s = 10^{-6}$ m s^{-1} (Figure 6, right). The evapotranspiration is ET = 0, 2, and 4 mm d^{-1}. By comparing the case of $\bar{h}$ = 0.3 m (low marsh) to the previous case of $\bar{h}$ = 0.6 m (high marsh), it may be seen that, as expected, aeration times decrease with decreasing $\bar{h}$, but the location of the preferential aeration zones as a function of K_s and ET remains about the same in most plots.

[29] In the low marsh the aeration times close to the surface (d = 0.10 m) are always higher than the corresponding values at d = 0.30 m, but, unlike the case of the high marsh, this happens both for the higher and the lower conductivity. Regardless of the mean elevation, if d = 0.10 m and $K_s = 10^{-5}$ m s^{-1}, no preferential aeration zone appears within the more conductive marsh and aeration times are invariant with respect to both ET and x. However, when the conductivity is low and ET = 0 mm d^{-1}, the location of the areas characterized by longer aeration times are near the channel edge, for both d = 0.10 m and d = 0.30 m. For higher ET values the aerated zone tends to migrate to the center of the marsh. In the lower marsh it is particularly evident that when $ET > 0$, the case of a lower conductivity is characterized by longer aeration times with respect to the case of higher conductivity. Indeed, when the conductivity is low, much greater pressure gradients are needed to support the flux toward the atmosphere required for deeper aeration layers and longer aeration times.

[30] In general, it is evident that our schematic salt marsh is divided into two zones, one near the channel and one located in its inner portion, with very different hydrologic characteristics. Channels act as drainage and recharge zones, creating patterns of preferential aeration zones where possibly plant growth takes place. The extension, depth, and persistence of the aeration zones depend on soil properties and on evapotranspiration (which is linked to the presence/absence of vegetation).

[31] If the conductivity is higher, the water flow regime is similar to the case of an island, with shorter aeration times along the sandy edges where vegetation hardly grows. Aeration times are higher in the center, but no aerated layer

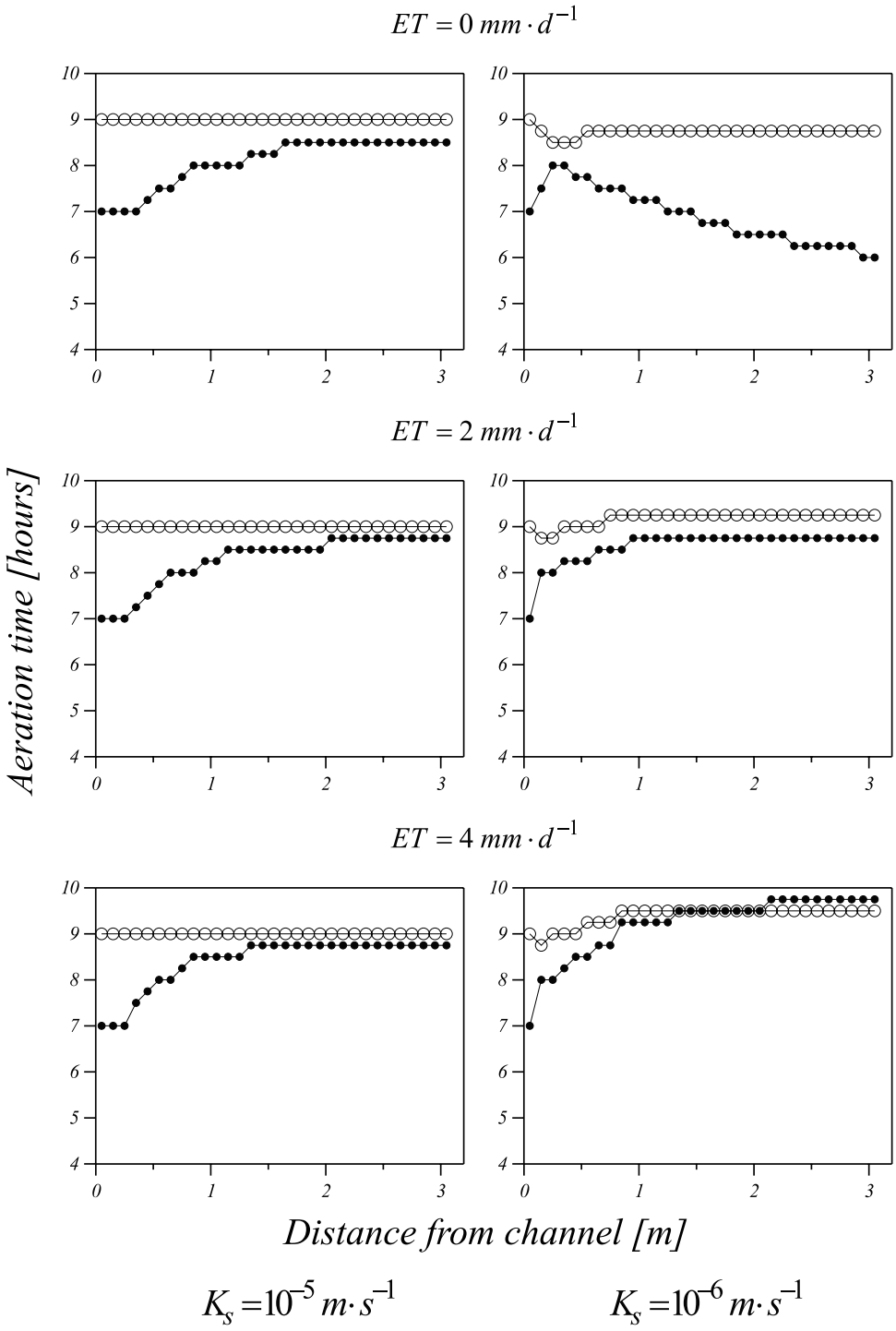

Figure 5. Aeration times as a function of the distance from the nearest channel for a marsh with mean elevation $\bar{h}$ = 0.6 m asl. The results for $K_s = 10^{-5}$ m s^{-1} and $K_s = 10^{-6}$ m s^{-1} are plotted on the left and on the right, respectively. The evapotranspiration is set to ET = 0, 2, and 4 mm d^{-1}. Aeration times for d = 0.10 are indicated with open circles, while solid circles refer to d = 0.30 m.

develops under the surface. Given the crucial role of oxygen for plant roots, vegetation in this case can only develop in the central area.

[32] When the conductivity is lower, the system becomes more similar to a real marsh: Subsurface water flow is very slow and, if ET = 0 mm d^{-1}, soils in the middle of the marsh are more saturated and a preferentially aerated zone develops close to the creek, where the soil is drained with the help of gravity and is more slowly recharged by the channels when the sea level rises. The situation drastically changes when evapotranspiration is increased uniformly over the whole surface: Aeration times are longer in the central part of the marsh, and the appearance of an unsaturated layer amplifies this phenomenon.

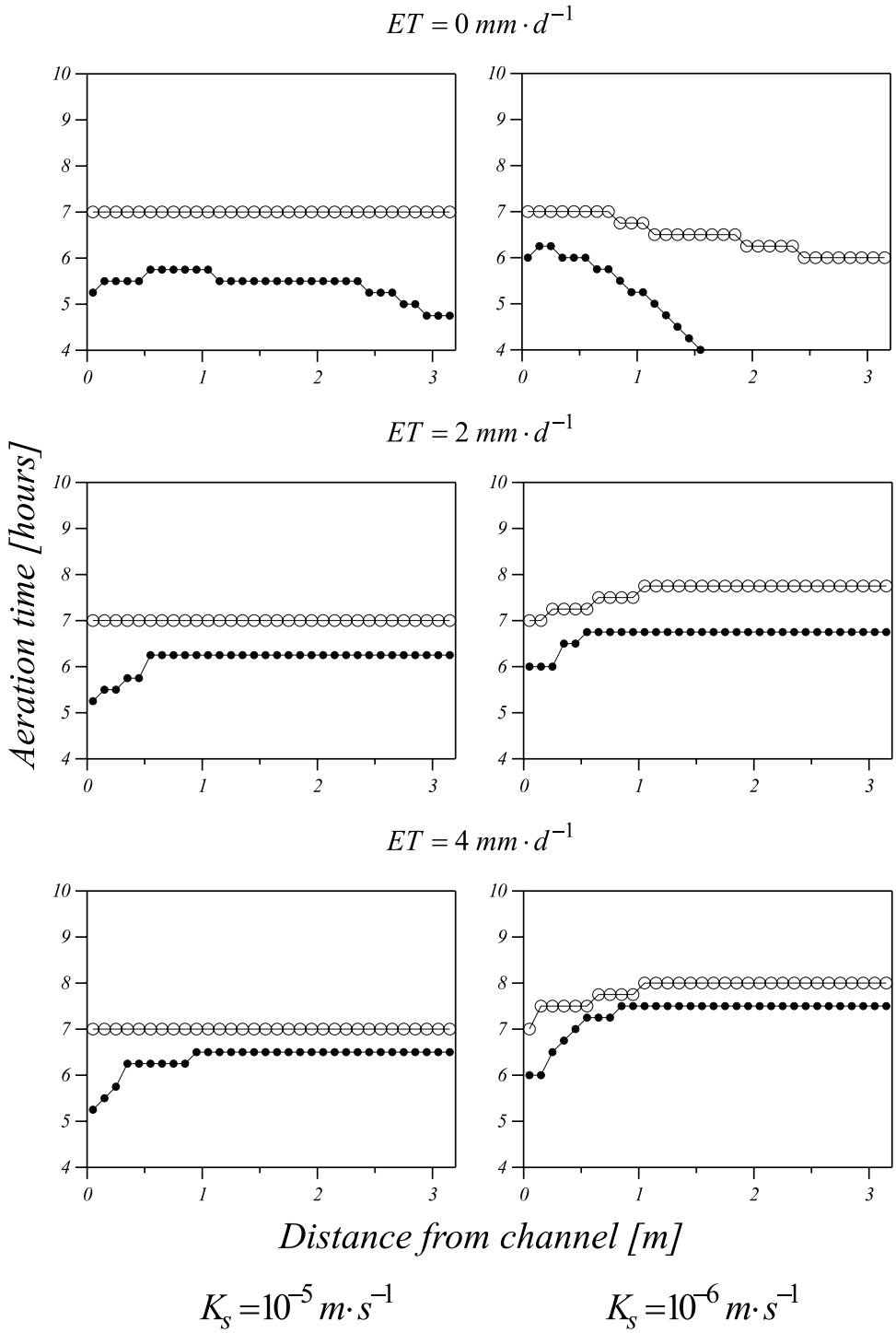

Figure 6. Aeration times as a function of the distance from the nearest channel for a marsh with mean elevation $\bar{h}$ = 0.3 m asl. The results for $K_s = 10^{-5}$ m s^{-1} and $K_s = 10^{-6}$ m s^{-1} are plotted on the left and on the right, respectively. The evapotranspiration is set to ET = 0, 2, and 4 mm d^{-1}. Aeration times for d = 0.10 are indicated with open circles, while solid circles refer to d = 0.30 m.

[33] If evapotranspiration values are associated with vegetation density, and thus with the degree of colonization of the salt marsh, different colonization scenarios may be represented and studied through different *ET* values. Considering, for example, a mud surface with no vegetation (and thus characterized by a very small *ET*), according to our model, plant colonization would start close to the channel, where the aeration times of soil layers are larger. This initial colonization would increase the evapotranspiration rate, thereby increasing aeration times and favoring a further colonization by plants less resistant to anaerobic conditions. When the whole surface of the marsh is homogeneously covered, the deep aerated layers will last longer and will lead to an increase in vegetation density in the

central part of the marsh because of a greater oxygen availability to the roots.

4. Conclusions

[34] Soil moisture dynamics relevant to plant establishment and growth in a salt marsh environment were discussed. The definition of a space−dependent aeration time was introduced to describe the relevance of the subsurface flow forced by tidal fluctuations and by evapotranspiration. Aeration times were evaluated numerically as a function of space (distance from the creek and depth) and hydrological factors (soil conductivity and evapotranspiration). Representative examples were discussed to demonstrate the existence of different flow regimes depending on conductivity and evapotranspiration values. The particular values of the parameters marking the transition between such regimes should be determined through more detailed modeling assumptions, but their existence may be expected to deeply influence the ecohydrology of real marshes, leading to moisture patterns similar to those obtained here for a schematic salt marsh.

[35] In summary, the analyses presented indicate that

[36] 1. Subsurface flow tends to be two-dimensional near the channels (both horizontal and vertical), whereas it is predominantly one-dimensional (vertical) away from it. The transition occurs within a few meters from the channel in all the soils considered in our simulations.

[37] 2. For evapotranspiration equal to zero, a lower hydraulic conductivity leads to greater soil aeration near the channel than in the middle of the marsh.

[38] 3. A uniform evapotranspiration reverses the pattern for a soil with low hydraulic conductivity: The more aerated zone migrates toward the inner part of the marsh.

[39] 4. A uniform evapotranspiration induces the formation of an aerated layer trapped underneath the flooded surface soil, thereby increasing the extent of the area where oxygen is available as well as its duration.

[40] 5. Deeper soil layers may be better aerated than shallower layers because of the presence of a ''trapped'' unsaturated zone induced by evapotranspiration.

[41] 6. Similar aeration times were found for marshes with a fixed value of saturated conductivity but with different mean elevations and thus different hydroperiods.

[42] The spatial and temporal soil moisture patterns described here have important implications for plant development and spatial organization and suggest a number of hypotheses regarding the colonization of salt marsh environments by vegetation. The unsaturated layer is more dynamic along marsh edges, where a two-dimensional flow field is induced by the channels that function as drains and sources during the fluctuations of the sea level. At some distance from the channels (which depends on soil conductivity and elevation) the water flow becomes predominantly vertical. If soil conductivity is low and evapotranspiration is small, the soil in the center of the marsh may be saturated for long periods of time, creating environmental conditions that cannot sustain plant development, even if downward fluxes are not hampered by any impermeable boundary. Whenever pioneer plants, resistant to severely anoxic conditions, may grow, they increase evapotranspiration rates and thus oxygen availability, creating a more favorable environment for the development of other vegetation species and affecting the location of the more aerated layers. The presence of vegetation over the surface of the marsh thus produces a strong positive feedback: The aerated soil layer, because of the enhanced evapotranspiration, lasts longer and reaches greater depths, allowing a prolonged presence of oxygen for aerobic root respiration.

[43] The schematic marsh model described here incorporates the main dynamics present in a real marsh soil and allows the description of the main ecohydrological processes taking place in tidal marshes. It also allows the selective study of the roles of the different factors at work and leads to the identification of an important feedback between biotic and abiotic components of tidal environments.

[44] More detailed descriptions of actual marshes will require the incorporation of other factors here purposely neglected. Important factors to be considered in future models include marsh topographic characteristics and the effects of heterogeneities in soil properties (e.g., surface macropores due to bioturbation) and in the evapotranspiration fluxes. The development of more complete descriptions of marsh subsurface hydrology is indeed interesting from a purely scientific viewpoint and is useful in an applicative perspective (e.g., for marsh management and construction).

[45] **Acknowledgment.** This work was funded by TIDE EU project EVK3-CT-2001-00064 and by COFIN 2002 Morfodinamica Lagunare project.

References

Adam, P. (1990). *Saltmarsh Ecology*, 461 pp., Cambridge Univ. Press, New York.

Allen, J. R. L. (2000), Morphodynamics of Holocene salt marshes: A review sketch from the Atlantic and southern North Sea coasts of Europe, *Quat. Sci. Rev.*, *19*(17–18), 1155–1231.

Alvarez Rogel, J., R. Ortiz Silla, N. Vela de Oro, and F. Alcarez Ariza (2001), The application of the FAO and U.S. soil taxonomy systems to saline soils in relation to halophytic vegetation in SE Spain, *Catena*, *45*, 73–84.

Armstrong, W. (1982), Waterlogged soils, in *Environmental Plant Ecology*, 2nd ed., edited by J. R. Etherington, pp. 290–330, John Wiley, Hoboken, N. J.

Armstrong, W., E. J. Wright, S. Lyhte, and T. J. Gaynard (1985), Plant zonation and the effects of the spring-neap tidal cycle on soil aeration in a Humber salt marsh, *J. Ecol.*, *73*, 323–339.

Cantero, J. J., R. Leon, J. M. Cisneros, and A. Cantero (1998), Habitat structure and vegetation relationships in central Argentina salt marsh landscape, *Plant Ecol.*, *137*, 79–100.

Chapman, V. J. (1960), *Salt Marshes and Salt Deserts of the World*, Leonard Hill, London.

Chapman, V. J. (1964), *Coastal Vegetation*, Pergamon, New York.

Dacey, J. W. H., and B. L. Howes (1984), Water uptake controls water table movement and sediment oxidation in short spartina marsh, *Science*, *224*, 487–489.

Fagherazzi, S., A. Bortoluzzi, W. E. Dietrich, A. Adami, S. Lanzoni, M. Marani, and A. Rinaldo (1999), Tidal networks: 1. Automatic network extraction and preliminary scaling features from digital terrain maps, *Water Resour. Res.*, *35*, 3891–3904.

Fagherazzi, S., P. L. Wiberg, and A. D. Howard (2003), Tidal flow field in a small basin, *J. Geophys. Res.*, *108*(C3), 3071, doi:10.1029/2002JC001340.

Friedrichs, C. T., and J. E. Perry (2001), Tidal salt marsh morphodynamics, *J. Coastal Res.*, *27*, 7–37.

Gardner, W. R. (1958), Some steady state solutions of unsaturated moisture flow equations to applications to evaporation from a water table, *Soil Sci.*, *82*, 228–232.

Howes, B. L., R. W. Howarth, J. M. Teal, and I. Valiela (1981), Oxidation-reduction potential in a salt marsh: Spatial patterns and interaction with primary production, *Limnol. Oceanogr.*, *26*, 350–360.

Jiao, J. J., and Z. Tang (1999), An analytical solution of groundwater response to tidal fluctuation in a leaky confined aquifer, *Water Resour. Res.*, *35*, 747–752.

Kadlec, R. H., and R. L. Knight (1996), *Treatment Wetlands*, pp. 137–140, CRC Press, Boca Raton, Fla.

Levine, J. M., J. S. Brewer, and M. D. Bertness (1998), Nutrients, competition and plant zonation in a New England salt marsh, *J. Ecol.*, *86*, 285–292.

Li, H., and J. J. Jiao (2002), Analytical solutions of tidal groundwater flow in coastal two-aquifer system, *Adv. Water Resour.*, *25*, 417–426.

Li, L., D. A. Barry, F. Stagnitti, and J. Y. Parlange (2000), Groundwater waves in a coastal aquifer: A new governing equation including vertical effects and capillarity, *Water Resour. Res.*, *36*, 411–420.

Mahall, B. E., and R. B. Park (1976), The ecotone between Spartina foliosa Trin. and Salicornia virginica L. in salt marshes of northern San Francisco Bay. II. Soil water and salinity, *J. Ecol.*, *64*, 793–809.

Marani, M., S. Lanzoni, D. Zandolin, G. Seminara, and A. Rinaldo (2002), Tidal meanders, *Water Resour. Res.*, *38*(11), 1225, doi:10.1029/2001WR000404.

Marani, M., E. Belluco, A. D'Alpaos, A. Defina, S. Lanzoni, and A. Rinaldo (2003), The drainage density of tidal networks, *Water Resour. Res.*, *39*(2), 1040, doi:10.1029/2001WR001051.

Marani, M., S. Lanzoni, S. Silvestri, and A. Rinaldo (2004), Tidal landforms, patterns of halophytic vegetation and the fate of the lagoon of Venice, *J. Mar. Syst.*, in press.

Mendelsshon, I. A., K. L. McKee, and W. H. Patrick (1981), Oxygen deficiency in Spartina alterniflora roots: Metabolic adaptation to anoxia, *Science*, *214*, 439–441.

Olff, H., J. P. Bakker, and L. F. M. Fresco (1988), The effect of fluctuations in tidal inundation frequency on salt-marsh vegetation, *Vegetatio*, *78*, 13–19.

Pezeshki, S. R. (2001), Wetland plant responses to soil flooding, *Environ. Exp. Bot.*, *46*, 299–312.

Philip, J. R. (1969), Theory of infiltration, *Adv. Hydrosci.*, *5*, 215–296.

Pignatti, S. (1966), *La Vegetazione Alofila della Laguna Veneta, Ist. Veneto di Sci., Lett. ed Arti Memorie*, *33*(1), 174 pp., Ist. Veneto di Sci., Lett. ed Arti, Venice, Italy.

Pullan, A. (1990), The quasilinear approximation for unsaturated porous media, *Water Resour. Res.*, *26*, 1219–1234.

Rinaldo, A., S. Fagherazzi, S. Lanzoni, M. Marani, and W. E. Dietrich (1999a), Tidal networks: 2. Watershed delineation and comparative network morphology, *Water Resour. Res.*, *35*, 3905–3917.

Rinaldo, A., S. Fagherazzi, S. Lanzoni, M. Marani, and W. E. Dietrich (1999b), Tidal networks: 3. Landscape-forming discharges and studies in empirical geomorphic relationships, *Water Resour. Res.*, *35*, 3919–3929.

Rogel, J. Á., R. O. Silla, and F. A. Ariza (2001), Edaphic characterization and soil ionic composition influencing plant zonation in a semiarid Mediterranean salt marsh, *Geoderma*, *99*, 81–98.

Russo, D. (1998), Stochastic modeling of scale dependent macrodispersion in the vadose zone, in *Scale Dependence and Scale Invariance in Hydrology*, edited by G. Sposito, pp. 266–290, Cambridge Univ. Press, New York.

Sanchez, J. M., J. Izco, and M. Medrano (1996), Relationships between vegetation zonation and altitude in a salt-marsh system in northwest Spain, *J. Vegetation Sci.*, *7*, 695–702.

Silvestri, S. (2000), La vegetazione alofila quale indicatore morfologico negli ambienti a marea, Ph.D. thesis, Univ. of Padova, Padua, Italy.

Silvestri, S., M. Marani, A. Rinaldo, and A. Marani (2000), *Vegetazione Alofila e Morfologia Lagunare*, Atti dell'Ist. Veneto di Sci., Lett. ed Arti, Venice, Italy.

Silvestri, S., A. Defina, and M. Marani (2004), Tidal regime, salinity and salt-marsh plant zonation, submitted.

Simonini, P., and S. Cola (2002), Some pore pressure measurements at the marsh of S. Felice in the Venice lagoon, in *Scientific Research and Safeguarding of Venice*, CORILA Research Program 2001 Results, Ist. Veneto di Sci. Lett. ed Arti, Venice, Italy.

Snow, A. A., and S. W. Vince (1984), Plant zonation in an Alaskan salt marsh. II. An experimental study of the role of edaphic conditions, *J. Ecol.*, *72*, 669–684.

Sun, H. (1997), A two-dimensional analytical solution of groundwater response to tidal loading in an estuary, *Water Resour. Res.*, *33*, 1429–1435.

van Genuchten, M. T. (1980), A closed-form equation for predicting the hydraulic conductivity of unsaturated soils, *Soil Sci. Soc. Am. J.*, *44*, 892–898.

Vince, S. W., and A. A. Snow (1984), Plant zonation in an Alaskan salt marsh. Distribution. I., abundance and environmental factors, *J. Ecol.*, *72*, 651–667.

Visser, E. J. W., T. D. Colmer, C. W. P. M. Blom, and L. A. C. J. Voesenek (2000), Changes in growth, porosity, and radial oxygen loss from adventitious roots of selected mono- and dicotyledonous wetland species with contrasting types of aerenchyma, *Plant Cell Environ.*, *23*, 1237–1245.

Vrugt, J. A., M. T. van Wijk, J. W. Hopmans, and J. Simunek (2001), One-, two-, and three-dimensional root water uptake functions for transient modeling, *Water Resour. Res.*, *37*, 2457–2470.

Yeh, T.-C. J. (1998), Scale issues of heterogeneity in vadose-zone hydrology, in *Scale Dependence and Scale Invariance in Hydrology*, edited by G. Sposito, pp. 224–265, Cambridge Univ. Press, New York.

M. Marani (corresponding author) and N. Ursino, Dept. IMAGE, University of Padova, via Loredan 20, I-35131, Padova, Italy. (marani@idra.unipd.it; nadia@idra.unipd.it)

S. Silvestri, Servizio Informativo del Consorzio Venezia Nuova, Campo S. Stefano, S. Marco 2949, I-30124, Venezia, Italy. (sonia@unive.it)